# Formation of Flower- or Cake-Shaped Stereocomplex Particles from the Stereo Multiblock Copoly(*rac*-lactide)s

Junli Hu, Zhaohui Tang, Xueyu Qiu, Xuan Pang, Yongkun Yang, Xuesi Chen,* and Xiabin Jing

*State Key Laboratory of Polymer Physics and Chemistry, Changchun Institute of Applied Chemistry, Chinese Academy of Sciences, Changchun 130022, China, and Graduate School of Chinese Academy of Sciences, Beijing 100039, China*

*Received May 18, 2005; Revised Manuscript Received June 17, 2005*

Flower- or cake-shaped particles with uniform particle size ranging from nanometers to micrometers were prepared from the stereo multiblock copoly(*rac*-lactide)s (smb-PLAs) by precipitating the polymer from its solution in methylene chloride/ethanol via three different methods: slowly lowering the solution temperature, slowly evaporating the solvent, and slowly adding a nonsolvent. Under the same condition, sheet-shaped crystals in 10 $\mu$m size but not particles were obtained from the pure PLLA with almost the same molecular weight. Electron diffraction and WAXD data demonstrated that the stereocomplex particles belonged to the monoclinic system. All three methods resulted in particles with identical morphology and almost the same particle size. At a given stereoregularity of 88%, as the molecular weight of the polymer increased from 8700 to 23 200 Da, the crystallinity decreased, the particle morphology changed from flower-shaped to cake-shaped, and the diameter and height of the particles increased from 0.8 and 0.45 to 3.6 $\mu$m and 2.0 $\mu$m, respectively. The initial concentration of the polymer solution influenced the particle size slightly but affected the morphology markedly. On the basis of the above experimental observations, it was proposed that the smb-PLA particles of flower- or cake-shape were formed in four steps: (1) complexation in solution of the smb-PLA chains; (2) particle nucleation; (3) particle growth in the width direction; and (4) particle growth in the height direction. The curvature of the paired smb-PLA chains and the inner stress governed the particle size, and the interconnection between the neighboring particles determined the layered structure and the package density of the particles formed.



## Introduction

Poly(lactide)s (PLAs) have received great attention in recent years due to their good biocompatibility, biodegradability, and potential applications in the medical field[1] as well as their industrial applications as a "green plastic".[2] Lactides have three different stereoisomers, that is, L-lactide, D-lactide, and *meso*-lactide. Racemic lactide (*rac*-LA) is a 1:1 mixture of L-lactide and D-lactide. Thus, poly(lactide)s may be poly(L-lactide) (PLLA), poly(D-lactide) (PDLA), poly(*meso*-lactide), and poly(*rac*-lactide), correspondingly. These polymers exhibit various physical and chemical properties due to their different stereostructures. Interestingly, when PLLA and PDLA are mixed at the ratio of 1:1, a unique composite is formed. It has a melting temperature ($T_m$) 50 °C higher than that of PLLA or PDLA, and it exhibits absolutely different X-ray diffraction peaks. This composite was referred to as a stereocomplex of PLLA and PDLA by Ikada et al.[3] Subsequently, comprehensive and intensive research on the stereocomplex was well done by this group. They prepared the stereocomplexes by various methods, such as forming in a concentrated solution,[4] casting blend film from a dilute solution,[5] crystallizing from melt,[6] and recrystallizing from an acetonitrile solution.[7] Stereocomplexes were also found in a binary blend film from a D-rich PLA and an L-rich PLA.[8] The later research showed that the stereocomplexes were also obtained by blending the polymers containing the PLLA sequence and those containing the PDLA sequence, provided that the stereoregular sequence length of each was long enough (more than 7 lactic acid units).[9−11]

During the past decade, the stereoselective polymerization of *rac*-LA has become a new interest of the polymer researches.[12−14] PLAs are usually synthesized by ring-opening polymerization of lactides with various metal catalysts.[15,16] The stereo multiblock copoly(*rac*-lactide)s (smb-PLAs) (see Figure 1) were synthesized by the stereoselective catalysts.[12,13] When the catalyst stereoselectivity is high enough, the stereoregular blocks of PLLA and PDLA will be long enough to form the crystalline stereocomplexes, as evidenced by the increase of $T_m$ and WAXD data in comparison with those of the pure PLLA and PDLA.[12]

The stereocomplexes obtained from the stereo multiblock copolymers have broader potential application due to their potential unique characters different from those of PLLA or PDLA. Yet, to date, most works focused on improving the stereoselectivity of catalysts and studying the mechanism of catalysis. Little research was given to the properties of the resultant polymers and their applications.

* To whom correspondence should be addressed. Tel.: +86-431-5262112. E-mail: xschen@ciac.jl.cn.

10.1021/bm050340i CCC: $30.25 
Published on Web 07/27/2005

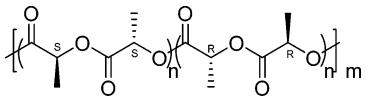

**Figure 1.** Structure of stereo multiblock copoly(*rac*-lactide).

Biodegradable nanoparticles and microparticles are potential candidates for controlled parenteral drug delivery due to their small particle size. They can protect protein from being degraded by enzyme present in gastrointestinal tract, ocular, and nasal delivery, and reduce the side effect of anticancer drugs to splanchnic organs such as liver and kidney. In addition, as compared to films and scaffolds encapsulating drug and growth factor for operation that involves implanting into the body, nanoparticles and microparticles for parenteral delivery are more convenient.

Recently, our group synthesized a series of stereoselective aluminum/Schiff base complex catalysts for the polymerization of *rac*-LA with a stereoselectivity as high as 90%.[12,17] Correspondingly, a series of stereo multiblock copoly(*rac*-lactide)s with high stereoregularity were obtained. In the present paper, the structure and properties of these smb-PLAs were studied by DSC, WAXD, and SEM, and flower- or cake-shaped particles with uniform particle size ranged from nanometers to micrometers were prepared from the smb-PLAs. Under the same conditions, only larger sheet crystals but not particles were obtained from the pure PLLA.

## Experimental Section

**Materials.** smb-PLAs were synthesized by the polymerization of *rac*-LA with [2,2-dimethyl-1,3-propylene bis(3,5-di-*tert*-butylsalicylideneiminato)] ethyl aluminum(III) as catalyst and 2-propanol as initiator.[12] PLLA ($M_n = 8500$ Da) was synthesized by the polymerization of L-lactide at 120 °C with stannous octoate as catalyst. The polymer was precipitated in cold methanol and filtrated, and then dried under vacuum at room temperature for 24 h. Their number-average molecular weight of the polymers ($M_n$) was evaluated in the chloroform solution by gel-permeation chromatography (GPC) with a Waters instrument (515 HPLC pump) equipped with a Wyatt interferometric refractometer, using polystyrene standards and calculated according to the formula $M_n = 0.58M_n$, GPC.[18] The parameter defining the stereoselectivity of the catalyst *P*m (*P*m is the probability of meso linkages) was determined from the relative tetrad intensities of the methine region of poly(*rac*-LA) in the homonuclear decoupled $^1$H NMR spectrum as follows:[19] [mmm] = $P\text{m}^2$ + (1 − *P*m)*P*m/2, [mmr] = [rmm] = (1 − *P*m)*P*m, [rmr] = (1 − *P*m)$^2$, and [mrm] = [(1 − *P*m)$^2$ + *P*m(1 − *P*m)]/2. The average number of the lactic acid units in the stereoregular blocks ($L_b$) is 2/(1 − *P*m).[20] The smb-PLA polymers synthesized were listed in Table 1.

**Measurements.** The polycrystal wide-angle X-ray diffraction (WAXD) of the smb-PLAs was measured using Rigaku D/max 2500kV PC X-ray diffractometer with Cu tube anode. The melting temperatures ($T_m$) and the fusion enthalpy ($\Delta H_f$) were measured by a Perkin-Elmer DSC-7 instrument, calibrated using indium as a standard. For the morphology observation of smb-PLA particles, their suspension was spin-coated on a piece of glass and then coated with a thin layer of gold prior to morphology observation by an environmental scanning electron microscope (ESEM, model XL 30 ESEM FEG from Micro FEI Philips). The sizes of the particles were the statistical average values of 100 particles measured form ESEM pictures, and their maximal standard deviation was 10%. Droplets of crystal suspension (0.05 wt %) in ethanol were deposited on carbon-coated grids and allowed to dry. These grids were sent to morphology and electron diffraction (ED) observation with a JEO2010 TEM electron microscope operated at an acceleration voltage of 200 kV.

**Table 1.** Raw Polymer Materials for the Preparation of smb-PLA Particles

| polymers | $M_n$ (Da) | *P*m | $L_b$ |
|---|---|---|---|
| smb-PLA$_{8.7k}$ | 8700 | 87.8% | 16.4 |
| smb-PLA$_{13.6k}$ | 13 600 | 88.6% | 17.5 |
| smb-PLA$_{23.2k}$ | 23 200 | 88.1% | 16.8 |

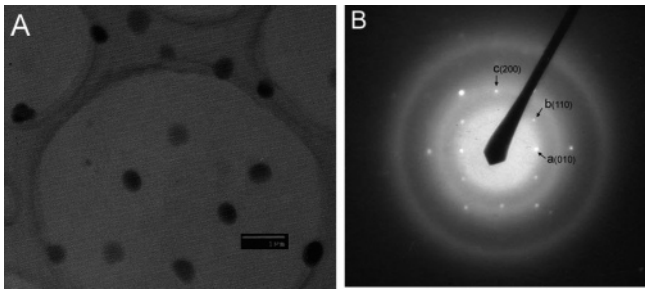


**Figure 2.** Transmission electron micrograph (A) and electron diffraction pattern (B) of the smb-PLA$_{8.7k}$ stereocomplex particles. [Solvent/nonsolvent ratio 50/120 (v/ v), initial polymer concentration 1 mg mL$^{-1}$, slowly evaporating the solvent.]

**Preparation of Stereocomplex Particles.** smb-PLA particles were prepared as follows. First, the polymer was dissolved in methylene chloride, and under moderate stirring a certain amount of absolute ethanol was slowly dropped into this solution to approach the saturation point of the polymer in the solvent/nonsolvent system at room temperature (20 °C). Second, the polymer was precipitated from the solution by one of three methods: (1) lowering the solution temperature to −20 °C and holding at this temperature for 24 h; (2) slowly evaporating the solvent methylene chloride at room temperature for 12 h; or (3) slowly adding the nonsolvent ethanol to the solution. Finally, the precipitate was collected by centrifugation for 10 min at room temperature (except for the first method, at −20 °C) and vacuum-drying.

## Results and Discussion

**(1) Electron Diffraction and WAXD Analyses.** Figure 2A showed the morphology of the smb-PLA$_{8.7k}$ particles prepared by the method of slowly evaporating the solvent. The round particles were about 800 nm in diameter. The wide-angle X-ray diffraction peaks (Figure 3, solid line) of the particles were typically the same as those of the PLLA/PDLA blend stereocomplexes.[3] The stereocomplexation of smb-PLAs occurred between the R-specific blocks and the S-specific blocks of the polymers. As discussed by Li liangbin et al., kinetically, forming homocrystals was more

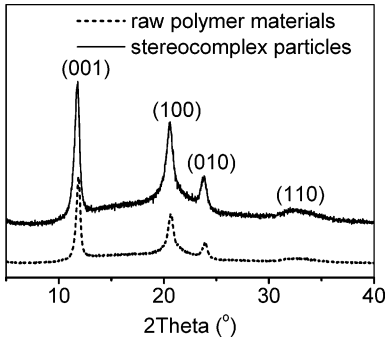


**Figure 3.** WAXD diagrams of smb-PLA$_{8.7k}$ raw polymer materials (dashed line) and the stereocomplex particles (solid line).

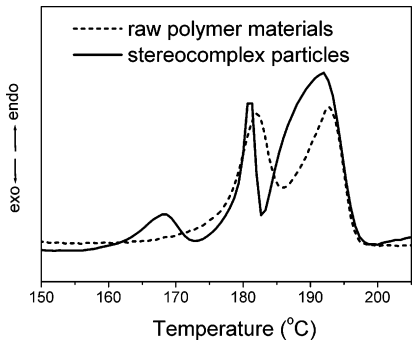


**Figure 4.** DSC traces of the smb-PLA$_{8.7k}$ raw polymer materials (dashed line) and the stereocomplex particles (solid line), heating rate 10 °C min$^{-1}$.

difficult than forming stereocomplexes.[21] As shown in Figure 2B, the electron diffraction spots of the smb-PLA$_{8.7k}$ particles formed an orthorhombic two-dimensional point lattice. The Bragg spacing values of diffraction spots (a) and (c) calculated with Au calibration were 0.371 and 0.214 nm, respectively. The pattern was supposed to be $a^*b^*$ plane. Spots (a) and (c) corresponded to 010 and 200, respectively. Accordingly, $d_{010}$ and $d_{100}$ were equal to 0.371 and 0.428 nm, respectively. The respective $a$- and $b$-axes were $a = 0.428$ nm and $b = 0.371$ nm. The X-ray diffraction patterns agreed with ED results as demonstrated in Figure 3. There was another strong diffraction signal at 11.8° that can be indexed as 001 corresponding to the spacing 0.741 nm. Taking into account the repeating period 0.870 nm of PLLA $3_1$ helix in stereocomplexes of PLLA/PDLA blend,[22] the chain axis was not vertical to the $a^*b^*$ plane. Therefore, the smb-PLA stereocomplexes belonged to the monoclinic system and the $\beta$ was 59.2° approximately. In contrast, Okihaha et al.[22] and Lotz et al.[23] reported the triclinic and hexagonal unit cell of PLLA/PDLA blend stereocomplexes, respectively.

**(2) DSC and Real-Time WAXD Analyses.** The DSC data of the smb-PLA particles were shown in Figure 4 (solid line). The raw polymer materials had two melting peaks (Figure 4, dashed line), and the smb-PLA particles had three separate melting peaks at 168, 181, and 192 °C, respectively. Only one peak at 188 °C appeared in the second scan for the smb-PLA particles (data not shown). Multiple melting peaks are normal phenomena for crystalline polymers. Generally, there are three possibilities: (1) The sample contains different crystal structures, and each peak is attributed to a specific crystal structure; (2) there is only one crystal structure, but the crystals have different sizes and degrees of perfectness; and (3) during heating, the unstable crystals undergo a melting−recrystallization process. In most cases, the second and third possibilities may coexist and the second possibility is the precondition for the occurrence of the third one. Ikada et al. have reported about the double peaks of the stereocomplexes of the PLLA and PDLA formed in acetonitrile solution.[7] They attributed the DSC peaks to the second and third possibilities.

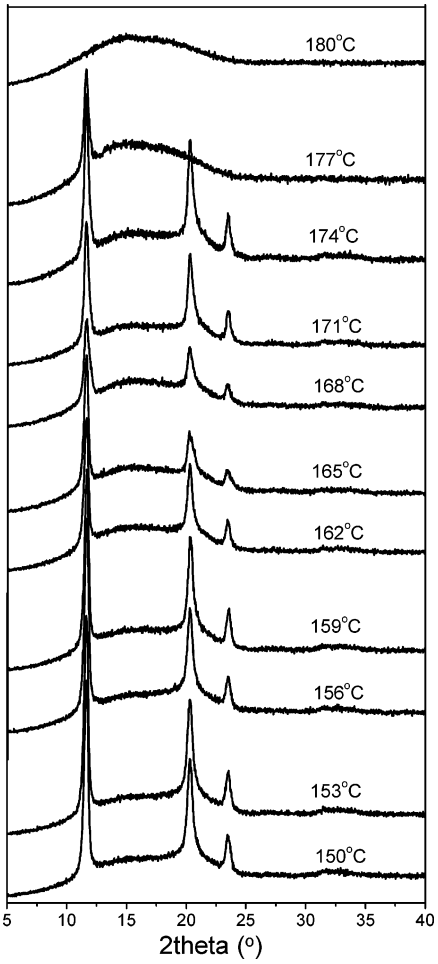


**Figure 5.** WAXD curves of the smb-PLA$_{8.7k}$ stereocomplex particles as a function of sample temperature. (Heating rate 10 °C min$^{-1}$, each temperature was held for 3 min before X-ray scanning, scan angle 5−40°, scan rate 8° min$^{-1}$.)

To identify the above possibilities, real-time WAXD curves of the smb-PLA particles were recorded from 150 to 180 °C in a step heating mode, as shown in Figure 5. Obviously, no new diffraction peaks appeared during the heating, suggesting that there was only one kind of crystal structure in the sample. Because the temperature-rising rate was much slower in WAXD measurement than that in DSC, it was reasonable that the melting temperature of the smb-PLAs determined by WAXD (180 °C) was much lower than that by DSC (194 °C). Figure 6 showed the variation of the diffraction intensities (areas) of 001, 100, and 010 peaks with the temperature. The three peaks showed a local minimum at 168 °C and a local maximum at 171 °C, while 100 and 010 peaks showed an additional minimum at 156 °C and maximum at 159 °C. Because the peak intensity was the measure of crystallinity in the sample, these minima and

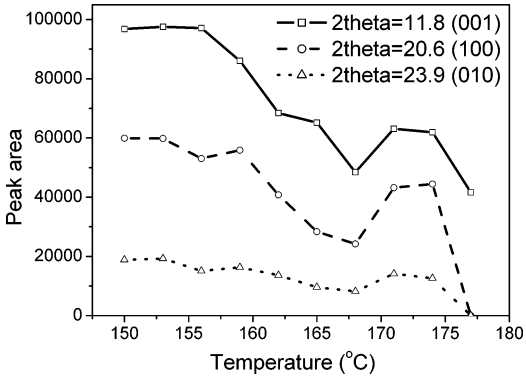


**Figure 6.** Plot of diffraction peak area against sample temperature for WAXD peaks with given crystallographic growth planes.

maxima indicated that a melting−recrystallization process took place during the heating. Similarly, the multiple peaks in DSC trace may be considered as the same process, that is to say, the less perfect crystals melted and recrystallized into more perfect crystals during the heating scan.

**(3) Particle Morphology and Size.** The morphology and size of the smb-PLA particles were examined by scanning electron microscopy. The particles were prepared by three different methods. To examine the influencing factors, different molecular weights of smb-PLA and initial polymer concentrations were used.

**(a) Effect of the Preparation Method.** Figure 7 showed the morphologies of the smb-PLA particles prepared via different methods using the same polymer materials smb-$PLA_{8.7k}$ at a solvent/nonsolvent ratio of 50/120 (v/v) and an initial polymer concentration of 1 mg $mL^{-1}$. The morphologies obtained from ESEM tallied with those from TEM. The three methods to precipitate the smb-PLA, that is, lowering the solution temperature, slowly evaporating the solvent, and slowly adding the nonsolvent, led to the same flower-shaped morphology, which was further composed of layered structures. Each layer had a thickness of about 50 nm. The particles looked flat and had a diameter *D* of around 700 nm in the width direction and a height *H* of around 400 nm in the thickness direction. The detailed data were listed in Table 2. It was seen that the three methods did not make a significant difference and all provided a favorable condition for the precipitation and crystallization of the smb-PLA molecules.

Similarly, Ikada et al. reported discoidal and spherical stereocomplex particles of PLLA/PDLA blend.[7] Besides, Domb et al. reported the porous spherical stereocomplex microparticles of enantiomeric lactic acid and sebacic acid triblock copolymers.[10] Although the shapes of these stereocomplex particles were different, their particle forming characters were the same. In a control experiment, the larger sheet crystals (data not shown) of about 10 $\mu$m were formed for pure PLLA with almost the same molecular weight ($M_n$ = 8500 Da) under the same conditions as those above (initial polymer concentration of 1 mg $mL^{-1}$, lowering the temperature). The different crystal shape of PLLA and smb-PLA was attributed to the different molecular chains package fashion in homopolymer crystals and stereocomplexes.

**(b) Effect of Molecular Weight of smb-PLA.** The effects of molecular weight of smb-PLA on the morphology and particle size were shown in Figure 8 and Table 3, respectively. The stereocomplex particles were prepared at the same conditions except the molecular weight of smb-PLA. As the molecular weight of smb-PLA increased from 8700 to 23 200 Da, the particle morphology changed from flower-shaped to cake-shaped and the diameter (*D*) increased markedly from 0.8 to 3.6 $\mu$m, and the height (*H*) from 0.45 to 2.4 $\mu$m. The cake-shaped particles had a smoother surface, but still had the layered structures. The sublayers were thicker and were packed at higher density than those in the flower-shaped particles. They were flat and round. In no circumstances was the shape of these particles spherical or discoidal. In contrast, the stereocomplex particles of the pure PLLA ($M_v$ = 27k) and PDLA ($M_v$ = 25k) blend had a discoidal shape of 4 $\mu$m diameter and 1 $\mu$m thickness formed from an acetonitrile solution of low polymer concentration or a spherical shape

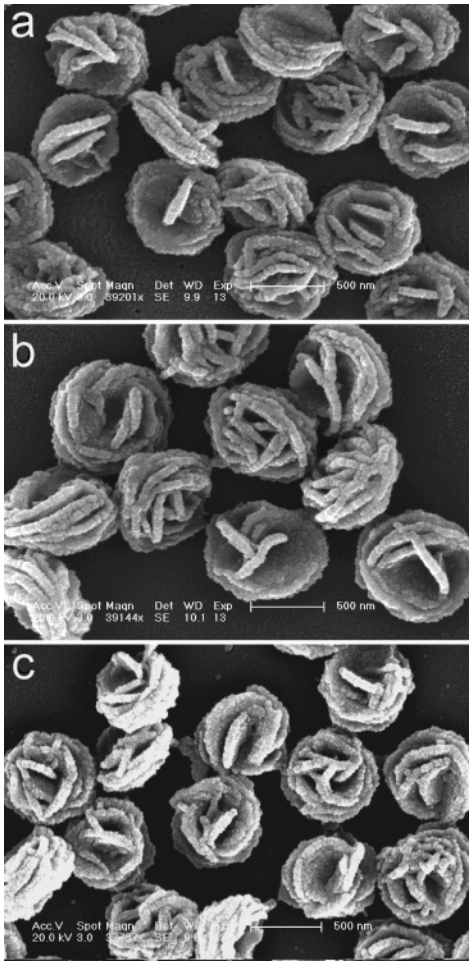


**Figure 7.** Morphologies of the stereocomplex particles prepared by different methods by ESEM. (a) Lowering solution temperature; (b) solvent evaporation; (c) nonsolvent addition. [Raw materials smb-$PLA_{8.7k}$, solvent/nonsolvent ratio 50/120 (v/v), initial polymer concentration 1 mg $mL^{-1}$.]

**Table 2.** Particle Sizes of smb-$PLA_{8.7k}$ Particles Prepared by Different Methods[a]

| preparation method | *D* (nm) | *H* (nm) |
|---|---|---|
| lowering solution temperature | 680 | 320 |
| slowly evaporating solvent | 800 | 460 |
| slowly adding nonsolvent | 670 | 430 |

[a] Preparation conditions were given in Figure 7.

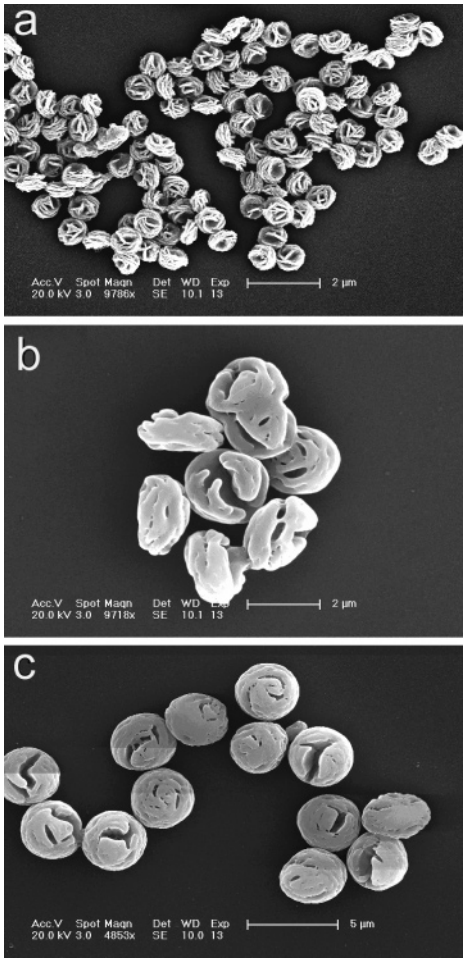


**Figure 8.** Effect of molecular weight on the morphology of the stereocomplex particles. (a) 8700 Da; (b) 13 600 Da; (c) 23 200 Da. [Solvent/nonsolvent ratio 50/120 (v/v), initial polymer concentration 1 mg mL$^{-1}$, solvent evaporation method.]

**Table 3.** Effect of the Molecular Weight on the Particle Size[a]

| molecular weight $M_n$ (Da) | $D$ (nm) | $H$ (nm) |
|---|---|---|
| 8700 | 800 | 460 |
| 13 600 | 2500 | 1200 |
| 23 200 | 3600 | 2350 |

[a] Preparation conditions were given in Figure 8.

of 4 $\mu$m diameter from a high concentration solution, as reported by Ikada et al.[7]

Figure 9 and Figure 10 showed the DSC and WAXD of the stereocomplex particles prepared from the smb-PLAs of different molecular weights. Evidently, at a given stereoregularity *P*m of 88%, the higher the molecular weight, the lower the $T_m$ and the weaker the diffraction intensity, indicating that as the molecular weight increases, the crystallinity and the crystal perfectness decrease. This is because the stereoregular block in a long molecular chain has difficulty forming a complex with its counterpart.

**(c) Effect of Initial Polymer Concentration.** The initial polymer concentration here refers to the polymer concentration in methylene chloride before ethanol's addition. As shown in Figure 11, with other conditions fixed, different polymer concentrations resulted in particles with different morphologies and sizes. The flower-shaped particles with *D* and *H* values of 680 and 320 nm were obtained at 1 mg

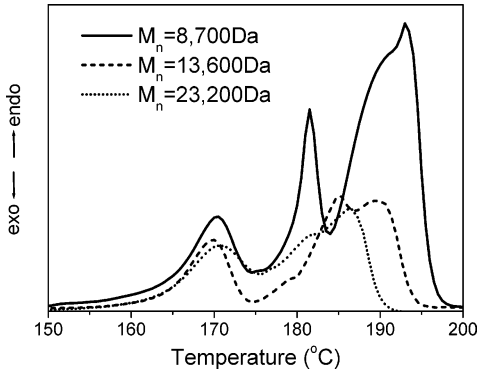


**Figure 9.** DSC traces of the stereocomplex particles prepared from smb-PLAs of different molecular weights. (Preparation conditions were given in Figure 8.)

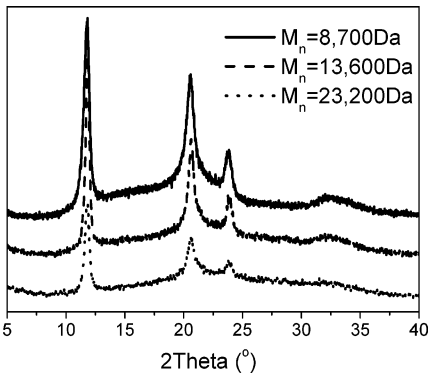


**Figure 10.** WAXD curves of the stereocomplex particles prepared from smb-PLAs of different molecular weights. (Preparation conditions were given in Figure 8.)

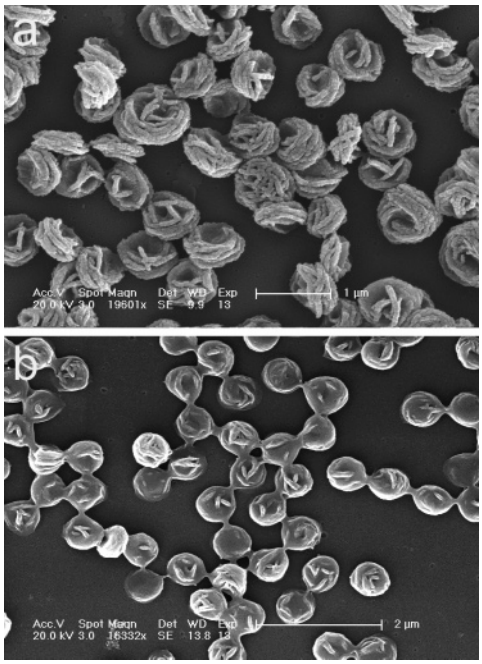


**Figure 11.** Effect of initial polymer concentration on the morphology of the stereocomplex particles. (a) 1 mg mL$^{-1}$; (b) 2 mg mL$^{-1}$. [Raw materials smb-PLA$_{8.7k}$, solvent/nonsolvent ratio 50/120 (v/v), lowering temperature method.]

mL$^{-1}$, and the cake-shaped particles with *D* and *H* values of 610 and 280 nm were obtained at 2 mg mL$^{-1}$. The particle sizes (*D* and *H*) decreased slightly with the concentration. This dependence on the polymer concentration was because

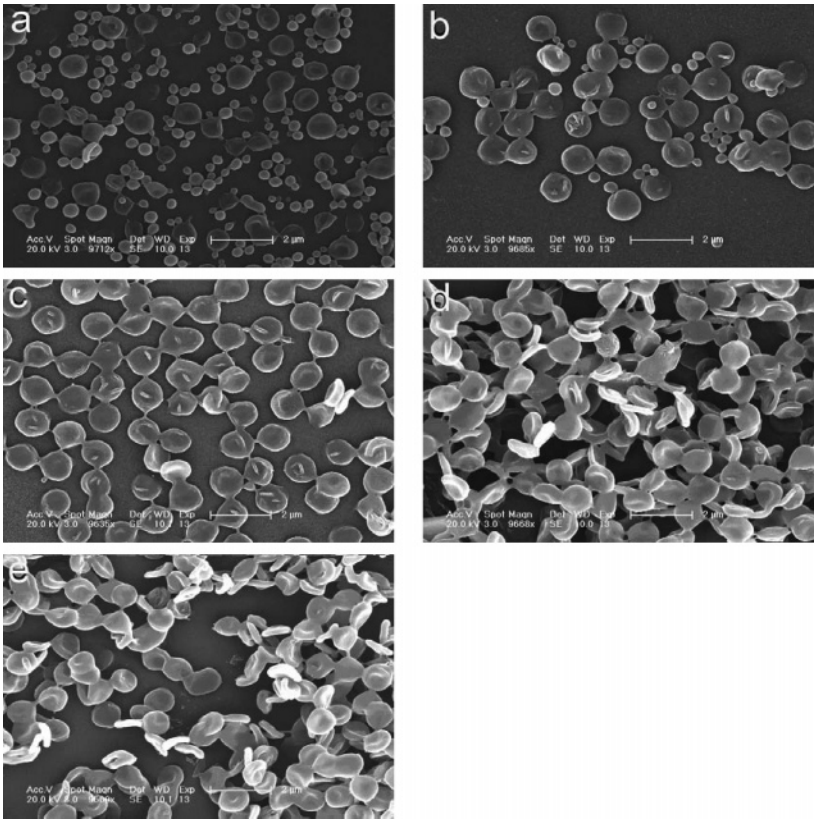


**Figure 12.** Morphologies of the stereocomplex crystals during the crystal growth process. (a) 5 min; (b) 10 min; (c) 35 min; (d) 100 min; (e) 18 h. The moment at which the solution became cloudy was taken as $t = 0$ min. [Raw materials smb-$PLA_{8.7k}$, solvent/nonsolvent ratio 50/120 (v/v), initial polymer concentration 4 mg $mL^{-1}$, solvent evaporation method.]

**Table 4.** Particle Sizes of the Stereocomplex Crystals during the Growth Process[a]

| *t* (min) | *D* (nm) | *H* (nm) |
|---|---|---|
| 5 | 150−1000 | 50−200 |
| 10 | 200−1000 | 50−250 |
| 35 | ~1000 | ~250 |
| 100 | ~1000 | ~300 |
| 1080 | ~1000 | ~300 |

[a] Preparation conditions were given in Figure 12.

the two steps of the particle formation, stereocomplexing and crystal growing, were both affected by the polymer concentration. Moreover, at 2 mg $mL^{-1}$ (Figure 11b), the most particles obtained were connected together in the width direction. This connection provided an indication that the stereocomplexed molecular chains could cross two particles.

**(4) Growth of the Stereocomplex Particles.** Figure 12 and Table 4 showed the variation of particle morphology and size with the growth time. The particles were prepared by the solvent evaporation method with smb-$PLA_{8.7k}$ and at the initial polymer concentration of 4 mg $mL^{-1}$. Here, the concentration was higher than that used for Figure 11b. Once again, cake-shaped particles were obtained finally. At the initial stage of the particle growth (0−10 min), the crystals grew in both width and height directions. Yet the growth stopped in the width direction and continued in the other direction after 35 min. In addition, the particle sizes were not uniform at the early stage but became uniform finally. This was because the crystal nuclei were not formed at the same time and the growth of a crystal was accompanied with the formation of a new nucleus. Because the driving force for the further growth of the particles was the inner stress in the twisted molecular chains of the stereocomplexes, the particles assumed a flat and round shape. As the diameter became larger and larger, the inner stress diminished. At a certain size, further growth would result in an increase of inner stress and consequently the particles stopped growing in the width direction, and another layer appeared and then began to grow, leading to the increase in height *H*. Once again, almost all particles were connected together in the width direction in Figure 12e. In Figure 12a and b, in fact, such connections were already observed between neighboring small particles. They might grow individually or merge into larger particles. In the former case, the interconnected particles could not grow in the same plane. This might be the reason for the layered structure of the particles.

It is noticed that the particles collected at 10 min (corresponding to Figure 12a) showed a DSC curve with $T_m$ peaks at 174.7, 185.3, and 194.6 °C and total enthalpies of fusion ($\Delta H_f$) of 56.2 J $g^{-1}$, and those collected at 18 h (corresponding to Figure 12e) showed $T_m$ peaks at 172.7, 183.3, and 193.4 °C and a total $\Delta H_f$ of 53.9 J $g^{-1}$. The WAXD curve (not shown) of the early product also showed strong diffraction peaks. This implies that the particles formed at the early stage were highly crystalline and those formed at the late stage had a little less crystallinity and crystal perfectness.

On the basis of particle shape, size, and growth process, and their dependence on molecular weight and initial concentration observed above, we can assume the formation mechanism of the flower- or cake-shaped smb-PLA particles.

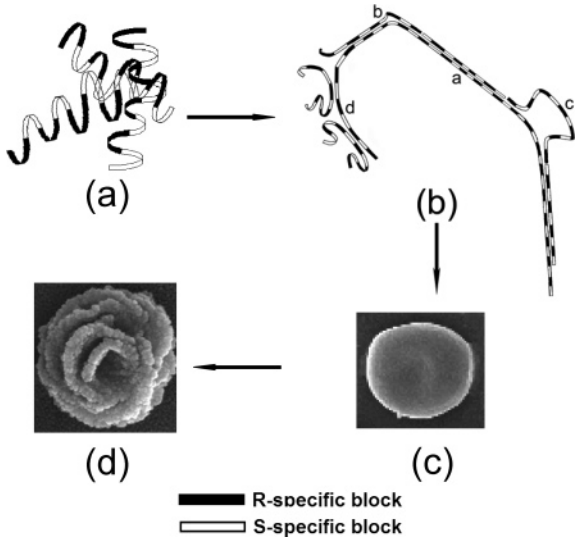


**Figure 13.** Mechanism for the formation of flower- or cake-shaped smb-PLA particles.

It might consist of four steps: (1) complexing − individual smb-PLA chains get complexed with each other in solution (Figure 13b); (2) nucleation − the complexed chains form the crystalline nucleus of solid state; (3) crystal growth in the width direction (Figure 13c); and (4) crystal growth in the height direction (Figure 13d). Similar to the stereocomplexes formed in a PLLA/PDLA blend,[22] the stereocomplexation in smb-PLA takes place between the R-specific block and S-specific block in parallel lateral fashion, as shown in Figure 13b, site a. Because the lengths of the stereospecific blocks are statistically equivalent but are not exactly identical, the nonmatching between the R-block and the S-block is more probable in smb-PLA than in the PLLA/PDLA blend and leads to formation of the faults in stereocomplexation, such as sudden bending or loops of various sizes, as shown in Figure 13b, sites b and c. Moreover, such stereocomplexation may occur between more than two molecules, and there are more structure faults as shown in Figure 13b, site d. Due to these structure faults, the paired chains trend to assume a bent shape with a certain curvature. When they are packaged into a crystal, inner stresses are caused, resulting in three features of the crystal growth in the width direction, that is, round shape, even size, and rough surface. These features are specific for smb-PLA. Under the similar conditions, pure PLLAs only form sheet-shaped crystals.

Before discussing the crystal growth in the height direction, let us look at an important experimental fact that the flat and round particles are connected together even when they are very small at the early stage as shown in Figure 12. Every particle trends to grow in its width direction. The confliction between two neighboring particles must result in the dislocation of their growing planes, leading to the growth in the height direction of the particle and the layered structure, as shown in Figure 13d. In each layer, of course, the growth is governed by the curvature of the paired chains and stops at a certain size. Undoubtedly, this growth in height direction shows more molecular weight dependency, because a pair of long chains may cross through more flat particles and their simultaneous growth will result in dense package in the final particle. Similarly, it depends on the solution concentration, because more crystal nuclei exist in the more concentrated solution. There is more probability for them to be tied together and to grow simultaneously in different directions.

## Conclusions

Flower- or cake-shaped stereocomplex particles of smb-PLAs with uniform particle size in the range of nanometers to micrometers were obtained by precipitating the polymer from the organic solution with different methods. Under the same condition, larger sheet-shaped crystals but not particles were obtained from the pure PLLA. The stereocomplex particles belonged to a monoclinic system different from the triclinic or hexagonal reported earlier for stereocomplexes of PLLA/PDLA blend. DSC of the particles exhibited three separate melting peaks due to a melting−recrystallization process of the relatively unstable crystallites during the heating scan. All three methods resulted in particles with identical morphology and almost the same particle size. At a given stereoregularity, as the molecular weight of the polymer increased, the crystallinity decreased, the particle morphology changed from flower-shaped to cake-shaped, and the size of stereocomplex particles increased. The initial polymer concentration in solvent influenced the particle size slightly but affected the morphology markedly. On the basis of the above experimental observations, it was proposed that the smb-PLA particles of flower- or cake-shape were formed in four steps: (1) complexation in solution of the smb-PLA chains; (2) particle nucleation; (3) particle growth in the width direction; and (4) particle growth in the height direction. The curvature of the paired smb-PLA chains and the inner stress governed the particle size, and the interconnection between the neighboring particles determined the layered structure and the package density of the particles formed.

These uniform stereocomplex microparticles are potential candidates for a drug delivery system due to their special ability of encapsulation, small particle size, and monodispersity. Further investigation is in progress.

**Acknowledgment.** This project is financially supported by the National Natural Science Foundation of China (Nos. 50273038, 20274048, 50373043), the National Fund for Distinguished Young Scholar (No. 50425309), and the "863" Project (2002AA326100) from the Ministry of Science and Technology of China.

## References and Notes

(1) Uhrich, K. E.; Cannizzaro, S. M.; Langer, R. S.; Shakesheff, K. M. *Chem. Rev.* **1999**, *99*, 3181−3198.
(2) Kirchhoff, M. M. *Environ. Sci. Technol.* **2003**, *37*, 5349−5353.
(3) Ikada, Y.; Jamshidi K.; Tsuji, H.; Hyon, S.-H. *Macromolecules* **1987**, *20*, 904−906.
(4) Tsuji, H.; Horii, F.; Hyon, S.-H.; Ikada, Y. *Macromolecules* **1991**, *24*, 2719−2724.
(5) Tsuji, H.; Hyon, S.-H.; Ikada, Y. *Macromolecules* **1991**, *24*, 5651−5656.
(6) Tsuji, H.; Hyon, S.-H.; Ikada, Y. *Macromolecules* **1993**, *26*, 6918−6926.
(7) Tsuji, H.; Hyon, S.-H.; Ikada, Y. *Macromolecules* **1992**, *25*, 2940−2946.

(8) Tsuji, H.; Ikada, Y. *Macromolecules* **1992**, *25*, 5719−5723.
(9) de Jong, S. J.; van Dijk-Wolthuis, W. N. E.; Kettenes-van den Bosch, J. J.; Schuyl, P. J. W.; Hennink, W. E. *Macromolecules* **1998**, *31*, 6397−6402.
(10) Slivniak, R.; Domb, A. J. *Biomacromolecules* **2002**, *3*, 754−760.
(11) Lim, D. W.; Chio, S. H.; Park, T. G. *Macromol. Rapid Commun.* **2000**, *21*, 464−471.
(12) Tang, Z. H.; Chen, X. S.; Pang, X.; Yang, Y. K.; Zhang, X. F.; Jing, X. B. *Biomacromolecules* **2004**, *5*, 965−970.
(13) Ovitt, T. M.; Coates, G. W. *J. Am. Chem. Soc.* **2002**, *124*, 1316−1326.
(14) Zhong, Z. Y.; Dijkstra, P. J.; Feijen, J. *J. Am. Chem. Soc.* **2003**, *125*, 11291−11298.
(15) Kricheldorf, H. R.; Berl, M.; Scharnagl, N. *Macromolecules* **1988**, *21*, 286−293.
(16) Montaudo, G.; Montaudo, M. S.; Puglisi, C.; Samperi, F.; Spassky, N.; LeBorgne, A.; Wisniewski, M. *Macromolecules* **1996**, *29*, 6461−6465.
(17) Tang, Z. H.; Chen, X. S.; Yang, Y. K.; Pang, X.; Sun, J. R.; Zhang X. F.; Jing, X. B. *J. Polym. Sci., Part A: Polym. Chem.* **2004**, *42*, 5974−5982.
(18) Baran, J.; Duda, A.; Kowalski, A.; Szymanski, R.; Penczek, S. *Macromol. Rapid Commun.* **1997**, *18*, 325−333.
(19) Chamberlain, B. M.; Cheng, M.; Moore, D. R.; Ovitt, T. M.; Lobkovsky, E. B.; Coates, G. W. *J. Am. Chem. Soc.* **2001**, *123*, 3229−3238.
(20) Coudane, J.; Ustrariz-Peyret, C.; Schwach, G.; Vert, M. *J. Polym. Sci., Part A: Polym. Chem.* **1997**, *35*, 1651−1658.
(21) Li, L. B.; Zhong, Z. Y.; de Jeu, W. H.; Dijkstra, P. J.; Feijin, J. *Macromolecules* **2004**, *37*, 8641−8646.
(22) Okihara, T.; Tsuji, M.; Kawaguchi, A.; Katayama, K.-I. *J. Macromol. Sci.,Phys.* **1991**, *B30*, 119−140.
(23) Cartier, L.; Okihara, T.; Lotz, B. *Macromolecules* **1997**, *30*, 6313−6322.

BM050340I